

Fracture strength of 3-units fixed partial dentures fabricated with metal-ceramic, graphene doped PMMA and PMMA before and after ageing: An in-vitro study

Original

Fracture strength of 3-units fixed partial dentures fabricated with metal-ceramic, graphene doped PMMA and PMMA before and after ageing: An in-vitro study / Ortensi, L.; Grande, F.; Testa, C.; Balma, A. M.; Pedraza, R.; Mussano, F.; La Rosa, G. R. M.; Pedulla, E.. - In: JOURNAL OF DENTISTRY. - ISSN 0300-5712. - 142:(2024).
[10.1016/j.jdent.2024.104865]

Availability:

This version is available at: 11583/2996274 since: 2025-01-06T22:47:07Z

Publisher:

Elsevier

Published

DOI:10.1016/j.jdent.2024.104865

Terms of use:

This article is made available under terms and conditions as specified in the corresponding bibliographic description in the repository

Publisher copyright

(Article begins on next page)

Fracture strength of 3-units fixed partial dentures fabricated with metal-ceramic, graphene doped PMMA and PMMA before and after ageing: An in-vitro study[☆]

Luca Ortensi^a, Francesco Grande^{a,b,*}, Claudia Testa^c, Alessandro Mosca Balma^d,
Riccardo Pedraza^{b,d}, Federico Mussano^d, Giusy Rita Maria La Rosa^c, Eugenio Pedullà^c

^a Department of Prosthodontics, University of Ferrara, Ferrara, Italy

^b Department of Mechanical and aerospace engineering, Polytechnic University of Turin, Turin, Italy

^c Department of General Surgery and Medical- Surgical Specialties, University of Catania, Italy

^d Department of Surgical Sciences, CIR Dental School, University of Turin, 10126 Turin, Italy

ARTICLE INFO

Keywords:

Three-units fixed partial dentures
Fracture load
G-CAM
Thermomechanical cycle

ABSTRACT

Objectives: To evaluate the fracture strength and linear elongation at break of three-units fixed partial dentures (FPDs) fabricated with traditional and new materials for fixed prosthodontics before and after ageing.

Methods: Sixty models of three-units FPDs were fabricated and cemented onto a Co-Cr model simulating the replacement of a maxillary second premolar. The samples were randomly divided into 3 groups: metal-ceramic (MCR), graphene-doped polymethylmethacrylate (PMMA-GR) and polymethylmethacrylate (PMMA). Half of the samples were directly subjected to fracture test, while the remaining half underwent an ageing process and then a fracture loading test using an electrodynamic testing machine. Fracture load and elongation at break values were taken and statistically analysed.

Results: Significant differences were detected between the different materials ($p < 0.05$). All groups showed a reduction of the fracture load and elongation at break values after ageing, but not statistically significant, except for PMMA group ($p = 2.012e-19$) ($p = 3.8e-11$).

Conclusions: MCR and PMMA-GR three-units FPDs showed higher fracture strength and lower elongation at break compared to PMMA. MCR and PMMA-GR had higher resistance to ageing processes compared to PMMA.

Clinical significance: PMMA-GR could be considered a material for long-term provisional restorations as its mechanical behaviour and ageing resistance are more like MCR than PMMA.

1. Introduction

The materials used for fixed prosthodontics are fundamental in determining the success of oral rehabilitation [1,2]. Depending on its mechanical, biological and aesthetic properties a given material may be considered suitable for either definitive or temporary three-unit fixed partial dentures (FPD) [3,4]. A series of options have become available in the past few years.

Consisting of a metal framework usually made of CoCr alloy (more rarely a noble alloy) coated by veneering porcelain ceramics, metal-ceramics [1] are the primary option for posterior FPDs and they are preferred to all-ceramic materials [5,6]. To develop a chemical bond

between metal and ceramic, the porcelain used is to have not only a sufficiently low sintering temperature, but also a Coefficient of Thermal Expansion (CTE) and a Coefficient of Thermal Contraction (CTC) compatible with those of the metal alloy [1]. Thus, a surface oxide layer of the base metals creates a chemical bond with the porcelain [1]. The bonding force can be influenced by the formulation of the alloy, its manufacturing technique and other factors such as the framework design that could be deformed at porcelain sintering temperatures [7]. Regarding the manufacturing techniques, CoCr frameworks for FPDs can be fabricated through both the conventional lost wax casting and the more recent computer-aided design/computer-aided manufacturing (CAD/CAM) [8–10]. The casting process is complex, and can determine

[☆] This work was not previously presented and received no financial support.

* Corresponding author at: Via Luigi Borsari 46, 44121 Ferrara, Italy.

E-mail addresses: francesco.grande@unife.it, s301918@studenti.polito.it (F. Grande).

the creation of rough surfaces and internal defects with uncontrollable dimensional accuracy of the prosthesis, which may hinder its mechanical performance [8]. CAD/CAM metal frameworks should be evaluated for mechanical properties like fracture strength, especially as regards the ceramic coating, since chipping represents the first mechanical complication of tooth supported FPDs [5,6].

Poly methyl methacrylate (PMMA) is a synthetic polymer conventionally prepared by free radical addition through chemical processes (powder/liquid) and polymerization of monomer methyl methacrylate [1,11]. During this process, a variable amount of uncured monomers in the final polymer inevitably remains, dependently on the operator and a series of parameters such as the quantity of monomer solution added, possible impurities thereof, ambient temperature, and pressure conditions [3,11]. The residual monomers may be associated with mucosal irritation, tissue inflammation, cytotoxicity, and reduced mechanical properties [12,13]. The reduced hardness and stiffness of conventionally fabricated PMMA makes it a short-term reliable material [14,15]. Furthermore, the poor antimicrobial property and porosity enhance the risk of polymer deterioration, which is in turn linked to the increased release of monomer as well as the onset of mucosal infections, sustained by *Candida albicans* and other pathogens [14,16]. PMMA blocks for CAD/CAM are instead industrially polymerized with optimized temperature and pressure, allowing the production of high-density polymers endowed with standardized superior mechanical properties, hardly influenced by the operator compared to conventional ones [3,17]. In addition, several strategies were also applied to ameliorate properties such as Young modulus, flexural strength and elongation at break, by incorporating different types of nanoparticles like titanium dioxide [18], silver/silica nanocarrier, and carbon nanotubes [19,20] in the PMMA structure.

In particular, the incorporation of nano-sized graphene oxides (nGO) (less than 1 wt%) into the formulation of polymeric materials has shown to improve considerably the material resistance in relation to weight and dimension [21], the elastic modulus, toughness, tensile and flexural strength, reducing, at the same time, the formation of clefs and their diffusion [22]. The tests of cytotoxicity and the reduced oxidative stress damage induced in human cells by these new materials compared to conventional PMMA made them eligible and safe for being used in the oral cavity [23]. Hence, the incorporation of graphene oxides (nGO) into PMMA has recently been applied in the dental field to fabricate complete and removable partial dentures, dental composites and fixed dental prosthesis on teeth and implants [24–26].

An increase in the antimicrobial properties of graphene-doped PMMA was also observed [27,28]. This property may be useful to prevent the occurrence of secondary caries and biodeterioration of the resin compounds in opposition to the lack of buffering capacity that affected polymeric materials [29], which leads to an enhanced growth of harbour acidogenic and acid-tolerant species [30,31]. In this sense, graphene-doped PMMA have shown interesting characteristics in exhibiting an anti-adhesive effect against microbial species in artificial saliva due to the presence of hydroxyl and carboxylic groups that, on the other side, improve the hydrophilicity of PMMA [27,28]. In this view, the amount of water absorbed by the material could be enhanced in presence of saliva and other fluids. However, no evaluation on the mechanical resistance of aged graphene-doped PMMA was found in literature on three-units FPDs especially in comparison to provisional and definitive restoration materials.

Then, the aim of this *in vitro* study was to evaluate the fracture strength of metal-ceramic, graphene-doped PMMA and PMMA CAD-CAM systems for three-units FPDs before and after ageing. The first null hypothesis was that there would be no differences in fracture strength and linear elongation at break amongst all the tested materials. The second null hypothesis was that there would be no differences in fracture strength and linear elongation at break between aged and non-aged materials.

2. Materials and methods

2.1. Digital design and manufacturing of the models

Sixty models with a first maxillary molar and a first premolar prepared for a three-units FPD were digitally designed and fabricated in cobalt-chromium alloy through industrial manufacturing (newAncorvis, Bargellino, Italy), using a five-axis milling machine (Mikron MILL S 400 U milling system, Biel, Switzerland). The abutments were distant 11.5 mm measured from the lateral preparation walls of the abutments, height 4.5 mm, the chamfer preparation width was 1 mm, the total occlusal convergence angle was 6° and the occlusal preparation design of the abutments was flat.

2.2. Digital design and manufacturing of the specimens

A sample size calculation was performed based on the study of Lopez-Suarez et al. [32] assuming 5% alpha error and 80% study power. Based on comparison of means, the required sample size was calculated to be 8 per group, increased to 10 to account for laboratory processing errors.

Sixty ($N = 60$) pieces simulating a three-units FPDs for the replacement of a second maxillary premolar were designed on a dental CAD software program (Exocad DentalCAD v3.1 Rijeka; exocad GmbH, Darmstadt, Germany) and milled by a five-axis milling machine (Mikron MILL S 400 U milling system, Biel, Switzerland) from prefabricated disks. The latter were constituted by a standard structure with round connectors of 9 mm² (3 × 3 mm), an internal space of 50 micrometers for the cement layer, similarly to other previous studies [32–34]. Conventional prefabricated teeth libraries for first maxillary premolar, second premolar and first molar from Exocad software were used for the occlusal design of the FPDs. Basing on the materials used and according to previous studies for sample calculation [32,33], three groups composed of twenty samples each were created:

- group 1 (MCR), representing the control group. A cobalt-chromium alloy was used (Magnum Solare, Mesa, Italy) and it was ceramic-veneered according to a ceramic moulding protocol for standardizing the construction phases [35]. During the CAD phase, to obtain the framework, 1.3 mm were cut back from the occlusal surface of the FPDs final design to leave space for the feldspathic ceramic coating (Super Porcelain EX-3, Kuraray Noritake, Frankfurt, Germany). This was subsequently printed on the cobalt-chromium framework using verticator (Transformer System, Udine, Italy) from the one FPD fabricated directly from the CAD design. The Magnum Solare is composed of Cobalt (Co) 66%, Chrome (Cr) 27%, Molybdenum (Mo) and 6% others Si, Mn. Its elastic modulus is 233 GPa, elongation at break of 11%, a solidus-liquidus temperature of 1307 ÷ 1417 °C, thermal expansion coefficient of (25 ÷ 500 °C) 14.3 × 10⁻⁶ K⁻¹ – (25 ÷ 600 °C) 14.5 × 10⁻⁶ K⁻¹, melting point of 1470 °C and maximum cooking temperature of 980 °C;
- group 2 (PMMA-GR). The graphene-doped PMMA disks (< 50 ppm) (G-CAM A3 type Monochroma by Graphenano Dental, Paterna, Valencia, Spain) were milled and then mechanical polished. G-CAM is a thermostable acrylic with a principal base of polymethylmethacrylate resin doped with graphene. The declared properties are: solubility 0.5 µg/mm³, water adsorption 4 µg/mm³, flexural strength 140±7% MPa, elastic modulus 3200±7% MPa, compressive strength 155±5 MPa, surface hardness of 88 Shore D and residual monomer <0.004% [36–38];
- group 3 (PMMA). The PMMA disks (Sinergia Disk and Block colour A3.5, Nobil Metal SpA) were used for milling and then mechanical polished. The Sinergia Disk is a 100% polymethylmethacrylate with a solubility in water < 1.7 µg/mm³, a water adsorption < 18 µg/mm³, flexural strength > 100 MPa and an elastic modulus > 2500 MPa [36–38].

2.3. Luting procedure

All the samples were cemented with a self-curing resinous cement (RelyX Unicem, 3 M, USA) using a standardized technique for each group here described:

- a. the abutments of the model were cleaned, dried and sandblasted with 50 μm aluminium oxide (Al_2O_3) particles (Polidental Ind. e Com. Ltda, Sao Paulo, Brazil). The substrate surface was then rinsed for 20 s and air-dried for 5 s. A thin layer of metal primer (Metal Primer Z, GC Dental, Tokyo, Japan) was placed on the surface with a disposable brush. The same treatment was performed for the inner portions of the MCR samples;
- b. the inner portions of the PMMA and PMMA-GR FDPs were treated with 30 μm silicon dioxide (CoJet-Sand, 3 M, St. Paul, USA), rinsed, air-dried and covered with a thin layer of bond (Clearfil Liner Bond, Kuraray Noritake, Frankfurt, Germany) that was subsequently polymerized for 40 s with a light-cured unit (XL 3000 – 3 M ESPE; light output: 500 mW/cm^2);
- c. a self-curing resinous cement (RelyX Unicem, 3 M, USA) was automatically mixed with its PTFE ring and placed on the internal part of the restorations;
- d. the three-units FPD was then placed on the corresponding dental model and all the complex was positioned in an electrodynamic testing machine (MTS Acumen 1 Electrodynamic Test System) that applied a constant force of 10 N above the central pit of the intermediate element for 5 min (Fig. 1);
- e. the excesses of luting agents were removed using a small brush;
- f. the models were all placed in a bath of distilled water for 48 h to obtain the complete cement polymerization.

Subsequently, one half of the sample ($n = 10$, half of every five sample groups) underwent thermal and mechanical cycles while the remaining 30 underwent directly through fracture loading test.

2.4. Ageing phase

The ageing phase consists of two steps. The first step consisted in placing the samples in a distilled water bath carrying out 30,000 thermal cycles from 5 to 55 $^{\circ}\text{C}$ with a dwell time of 30 s (Thermo-cycler The 1100/1200; SD Mechatronik GMBH, Feldkirchen- Westerham, Germany).

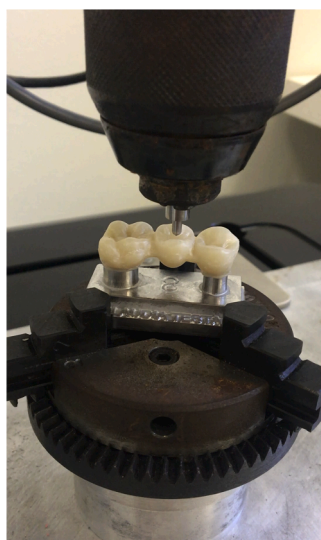


Fig. 1. Three-units FPD sample on the metal alloy base during the cementation phase.

In the second phase, the samples were fixed in the electrodynamic testing machine (MTS Acumen 1 Electrodynamic Test System) to perform 6550 mechanical cycles. A variable force from 40 N to 400 N at the frequency of 1.6 Hz was applied orthogonally to the occlusal plane according to the average occlusal force at maxillary premolars and molars positions [32,39,40].

The metal pin inserted into the electromechanical machine was held in place by a self-tightening chuck and measured:

- Total length: 23 mm;
- Tip length: 5 mm;
- Tip diameter: 2.5 mm;
- Rounded tip.

2.5. Fracture loading test

After the mechanical cycles, fracture was induced using a specific function of the MTS Acumen called “fracture load test” (Fig. 2). The machine used to carry out the mechanical and fracture tests was associated with a software (MTS Test Suite Multipurpose) that registered, organized and transferred the data relating to number of cycles and force value at which fracture occurred in an Excel file. In addition to this, the machine calculated the tip displacement in vertical direction related to the force exerted; this proved the linear elongation at break of the material, that represents the deformation of the sample before the fracture.

The fracture was registered by the electrodynamic testing machine in the moment of the drastic fall of the load curve and a visible breakage of the prosthesis occurred. For MCR group, only the fracture of the ceramic coating was considered. These values were organized in Excel (Office 16) and MATLAB R2022a for statistical processing.

2.6. Statistical analysis

The normal distribution of the sample was evaluated using the Shapiro-Wilk test. The Kruskal-Wallis non-parametric test with a post-hoc Bonferroni correction was performed to assess the statistical difference in fracture strength and elongation at break between the different materials and groups. A $p \leq 0.05$ was considered statistically significant. A Weibull modulus was also calculated to determine the reliability of the data before and after ageing. For brittle ceramic materials, the maximum stresses sustained by the samples before fracturing could vary. This variation is related to the presence of defects in the samples responsible for crack generation and, in turn, fractures. If the fracture load values are evenly distributed and show little variation,

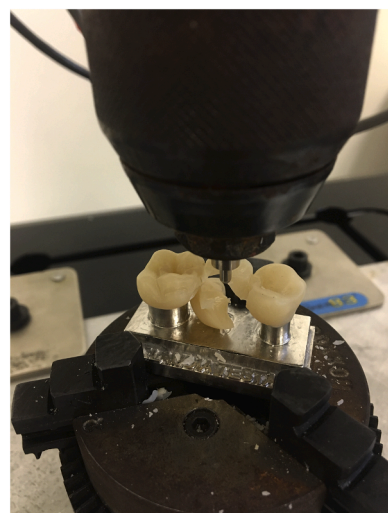


Fig. 2. Three-units FPD sample after fracture loading test.

then the Weibull modulus will be high. However, if the measured values exhibit higher variability and are not evenly distributed, the Weibull modulus will be lower.

3. Results

All FPDs survived thermal and mechanical cycles without showing cracks or fracture failures and underwent the fracture loading test. However, from the statistical analysis the following samples were excluded:

- Three samples from the aged PMMA, as they showed an elastic behaviour that determined the activation of the safety system by the testing machine during the mechanical cycles;
- three outliers, one from the aged MCR, one from not aged MCR and one from the not aged PMMA-GR, because their values were more than 1.5 interquartile ranges above the upper quartile or below the lower quartile.

Finally, 54 fractured samples underwent through statistical analysis.

Mean fracture load with their standard deviation values were 1304 ± 20 N for MCR, 1159 ± 74 N for PMMA-GR and 1286 ± 19 N for PMMA. The same values for aged materials were 1244 ± 10 , 1146 ± 70 , 269 ± 48 N for MCR, PMMA-GR and PMMA, respectively. Linear elongation at break values were 0.34 ± 0.08 mm for MCR, 1.04 ± 0.11 mm for PMMA-GR and 1.13 ± 0.17 mm for PMMA while for aged groups were 0.53 ± 0.25 , 1.05 ± 0.11 , 0.02 ± 0.13 mm. All these values were summarized in Table 1.

The Shapiro-Wilk test revealed that the average distribution was normal for PMMA-GR, aged PMMA-GR and aged PMMA but not for MCR groups and non-aged PMMA, so, a Kruskal-Wallis non-parametric test with a post-hoc Bonferroni correction was performed ($p = 0.05$). This test highlighted statistically significant differences between groups of materials both in fracture load and linear elongation at break values. MCR showed a statistically relevant higher fracture strength than PMMA ($P = 0.0004$) and PMMA-GR ($P = 0.0003$). A statistically significant difference was also observed between PMMA and PMMA-GR ($P = 0.0002$).

For linear elongation at break, MCR had a statistically lower values compared to PMMA-GR ($P = 0.0003$) and PMMA ($P = 0.0002$) and a significant difference was also found between PMMA-GR and PMMA ($P = 0.0275$).

All the materials revealed a reduction of the fracture load values after ageing; a statistically significant difference before and after ageing was found in MCR ($P = 0.0003$) and PMMA group ($p = 0.0006$). Only PMMA-GR did not show significant differences after thermocycling ($P = 0.5676$). The groups of materials differ to each other for fracture load values, even after ageing: MCR was significantly higher than PMMA-GR ($p = 0.0003$) and PMMA ($p = 0.0004$), while PMMA was significantly

lower than PMMA-GR ($p = 0.0002$).

After ageing, values of linear elongation at break raised for MCR and PMMA-GR while for PMMA reduced; a statistically significant difference before and after ageing was found for PMMA group ($p = 0.0006$), while no statistically relevant differences were found for MCR ($p = 0.1223$) and for PMMA-GR ($p = 0.7440$).

Comparing materials after ageing for the elongation at break, PMMA-GR showed significantly higher elongation than MCR ($p = 0.0003$) and PMMA ($p = 0.0275$), and PMMA was also significantly lower than MCR ($p = 0.0002$).

The Weibull modulus (Table 2), associated with an average resistance value, showed that PMMA-GR aged shows less variability in measurements respect to the same unaged material (Fig. 3). MCR follow the same trend, the Weibull modulus of the unaged ones is lower than the aged (Fig. 4). Regarding PMMA, an opposite behaviour was observed when compared to the other two materials (Fig. 5). After ageing process the Weibull modulus appears to be lower than the unaged samples resulting from a higher variability of the data.

4. Discussion

In this study, the fracture strength and the linear elongation at break values of metal-ceramic, graphene-doped PMMA and PMMA used for posterior three-units FPDs before and after thermocycling were evaluated.

Based on the results, the first and the second null hypotheses were rejected, since statistically significant differences across all the groups were detected. Fracture load values of MCR group were significantly higher than those obtained in the two resin groups both before and after ageing, as expected considering the higher mechanical properties of the ceramic material sustained by the metal framework [41]. The higher fracture strength of PMMA group compared to PMMA-GR, before ageing, could be explained by the fact that the filler raises the toughness, the flexural strength, the wear resistance and the elastic modulus [21] reducing, at the same time, the deformation under compressive load of the material that becomes more fragile. This was partially in accordance with another work where the tensile strength of non-aged G-CAM compared to that of PMMA was found to be only slightly increased [42], while in our study the difference was relevant.

Focusing on aged groups, MCR showed the highest value, followed by the PMMA-GR and, after a drastic decrease of fracture load value, by the PMMA. It is worth to note that, after ageing, all groups showed a decrease in fracture load values (Fig. 6). However, this decrease was not statistically significant for the PMMA-GR group compared to the non-aged group. This could explain that G-CAM is characterized by a significantly lower water sorption, solubility and elution than PMMA, as declared by the manufacturer, which leads to a greater conservation of the original mechanical properties of the material [42]. Furthermore, the reduced residual monomer release in comparison to conventional PMMA can be considered as an indirect indicator of an improved polymerization degree of the material that is strengthened by this process [43,44]. After ageing, PMMA samples showed a drastic fall of fracture resistance. This was probably due to the low long-term duration properties of the material which are considered as provisional in clinics. The water sorption and the solubility or leachability of resin materials may explain this behaviour in comparison to PMMA-GR and MCR [45,46]. In addition, MCR showed a statistically significant difference comparing aged and non-aged groups; yet this difference was significantly lower

Table 1

Trade name, composition of the materials, number of samples statistically evaluated, mean fracture load and elongation at break values.

	Group 1		Group 2		Group 3	
	Magnum Solare (MESA)		G-CAM (Graphenano Dental)		Sinergia Disk (Nobil Metal)	
	Cobalt-chromium alloy coated with felspathic ceramic		Graphene-doped polymethyl methacrylate		Polymethyl methacrylate	
	$n = 9$	$n = 9$ (Aged)	$n = 9$	$n = 10$ (Aged)	$n = 10$	$n = 7$ (Aged)
Fracture load (N)	1305 ± 2	1244 ± 1	1159 ± 74	1146 ± 70	1286 ± 19	269 ± 48
Elongation at break (mm)	0.34 ± 0.08	0.53 ± 0.25	1.04 ± 0.11	1.05 ± 0.11	1.13 ± 0.17	0.02 ± 0.13

Table 2

Weibull modulus for each group of material.

SAMPLE	PMMA-GR	MCR	PMMA	PMMA-GR Aged	MCR Aged	PMMA Aged
WEIBULL MODULUS	5	174.7	18.4	5.3	368.2	1.9

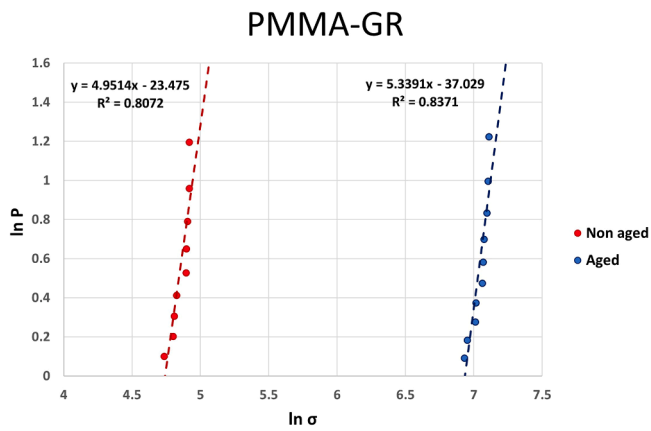


Fig. 3. Weibull modulus of the fracture load of PMMA-GR with aged and non-aged group.

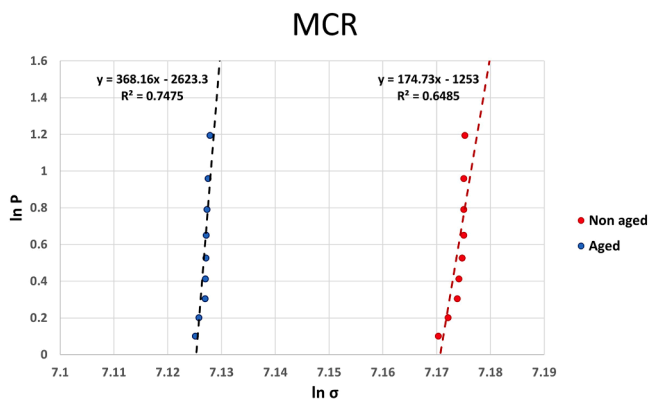


Fig. 4. Weibull modulus of the fracture load of MCR with aged and non-aged group.

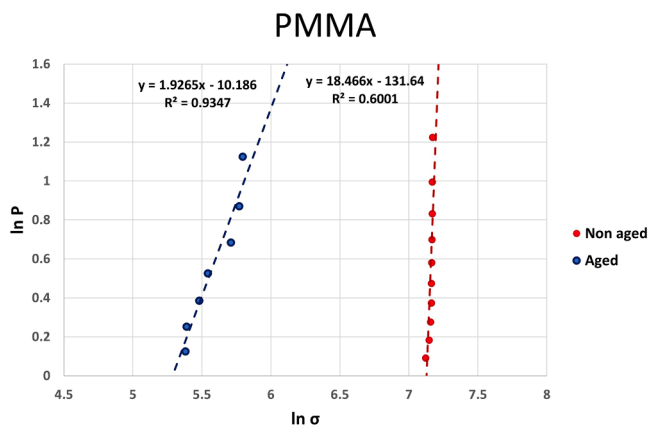


Fig. 5. Weibull modulus of the fracture load of PMMA with aged and non-aged group.

than that observed in PMMA and it could be speculated that the loss of mechanical properties did not owe to the MCR itself, but rather to the resin cements used. This consideration is also suggested by the fact that the abutment design used in this study maximizes the role of resinous cement in the fracture loading test [47,48]. However, as no specific analyses were conducted for evaluating this aspect, no certain conclusions can be driven on the matter.

In this study, the vertical displacement of the tip before fracture was also registered by the machine and assessed. It could be indirectly

considered as an indication of the maximum deformation of the sample and then of the malleability of the material [49,50]. As expected, before the ageing process, the MCR showed the lowest deformation values because of the elastic modulus of the ceramic coating [51]. However, it is interesting to underline that, before and after ageing, only PMMA and MCR groups showed changes of the “deformation” values before fracture (Fig. 7). For MCR groups, this behaviour may be linked with the softening of the resin cements after thermocycling [52,53]. As for PMMA, in addition to the cement softening, the excursion of the vertical tip was extremely low showing a more fragile fracture than the non-aged group, in line with the impairment of the mechanical properties of the material. This evidence correlates with the corresponding fracture loading values found before thermocycling. Interestingly, the PMMA-GR showed no difference before and after ageing in terms of deformation before fracture, in accordance with the loading values. This could be due to the enhanced polymerization process of the PMMA-GR which, therefore, leads to a higher stability of the polymer and to a reduced or absence of residual unpolymerized monomers leakage that is normally responsible for the water sorption phenomena [43,44]. Observing the fracture pattern of each material, the weak point of the PMMA-GR in this study was the connector, while for PMMA the fracture occurred especially in the mesio-distal direction. It can be speculated that this behaviour is probably related to the distribution of the graphene particles in PMMA matrix that changes the direction of cracks propagation along the filler-polymer interface [54,55]. However, in absence of a fractographic analysis, it is challenging to estimate the exact origin of the failure for each material and where the piston used generated some contact damages.

A previous in vitro study tested G-CAM to determine the influence of graphene on the mechanical properties [21]. The results showed that G-CAM had a statistically significant higher mechanical resistance in compression and a higher elastic modulus compared to conventional PMMA. No significant differences were observed in the coefficient of friction and hardness. In addition, an added graphene percentage of 0.027wt% was detected using RAMAN spectroscopy. This percentage guarantees a low material cost and satisfactory aesthetic performances for dental prosthodontic use. The results regarding mechanical properties are in accordance with our study.

Another study assessed the fracture resistance of five types of complete coverage crowns fabricated from different materials [56]. The results showed the doped PMMA had a fracture load quite equal to that obtained by a single crown of cubic zirconia and the fracture resistance value reported by the authors was also similar to that obtained in our study [56].

The results of this study are clinically relevant, since they suggest that PMMA-GR performs better than conventional PMMA in terms of fracture strength, especially after ageing. Therefore, it may be used as a material for long-term provisional of posterior maxillary FPDs with greater reliability compared to conventional PMMA. Its use as definitive restoration, however, ought to be assessed in further studies also assessing the colour stability of the material, a high number of mechanical cycles and different restoration designs.

This study presents some limitations: first its in vitro design. In the oral cavity, restorations are not only affected by vertical occlusal forces. Therefore, in addition to a single loading direction, a multi-axial composite load should also be performed. In addition, many studies used the thermocycling process to simulate ageing to evaluate the long-term success of prosthetic rehabilitations by using in vitro experiments [33, 57–59]. However, the great heterogeneity of materials and the oral environment make a real comparison difficult. Secondly, the absence of a fractographic analysis, as previously mentioned. Third, the preparation at 6° of the abutments in the clinical setting is a challenging task, prone to preparation undercuts [60]. This may have enhanced the retention and resistance of restorations fabricated and consequently affected the fracture resistance of the material itself [61].

Additionally, the ageing process and the loading cycles of the

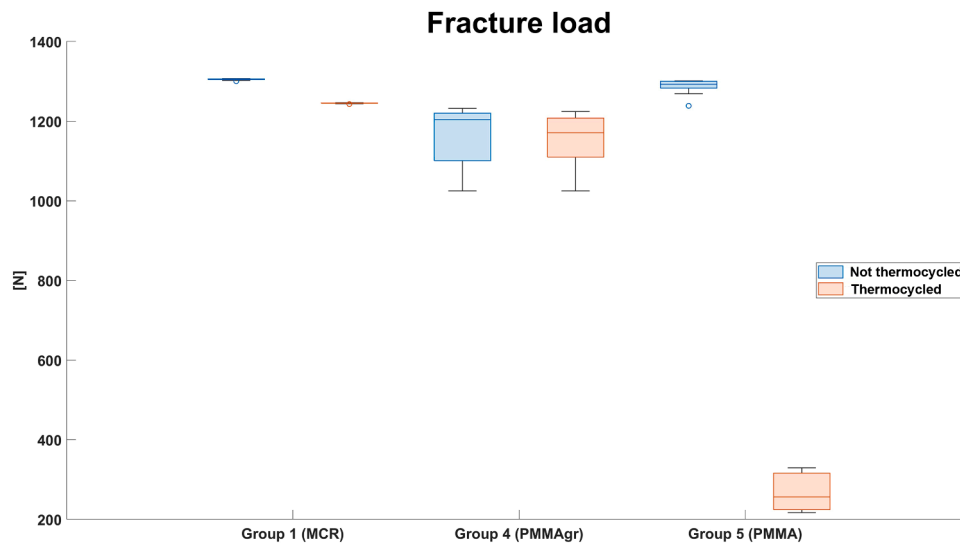


Fig. 6. Box plots representing fracture load values of the groups reported in Newton (N).

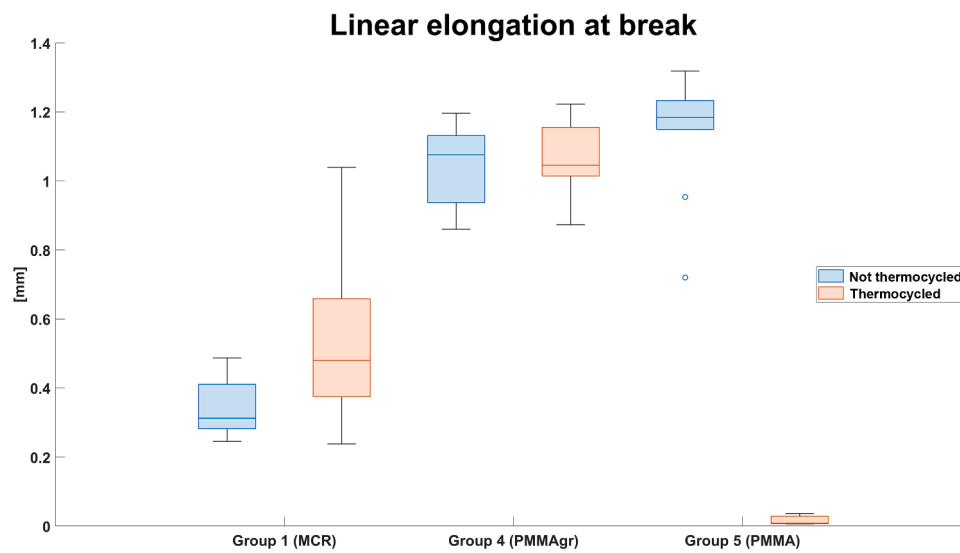


Fig. 7. Box plots representing linear elongation at break values of the groups reported in millimeters (mm).

samples were not performed simultaneously, and the type of material ageing may have also influenced the results [62]. The connector dimensions were standardized but as they influenced the fracture resistance of the material [3,63], it could be interesting also to evaluate smaller connectors. Additionally, in order to assess the influence of the luting agent on the fracture strength of the prosthesis, an evaluation of the bond strength of the cement used on each material after roughening should also be studied. This, in addition with a multiaxial loading, could be the focus of future in vitro research on this topic.

5. Conclusions

MCR and PMMA-GR showed higher mechanical properties than PMMA. MCR and PMMA-GR seemed not to be influenced by the ageing process. Mechanical properties of PMMA were significantly affected by the ageing process.

CRedit authorship contribution statement

Luca Ortensi: Visualization, Validation, Supervision, Resources,

Project administration, Conceptualization. **Francesco Grande:** Methodology, Writing – review & editing, Writing – original draft, Formal analysis, Data curation. **Claudia Testa:** Investigation. **Alessandro Mosca Balma:** Formal analysis, Data curation. **Riccardo Pedraza:** Writing – review & editing, Data curation. **Federico Mussano:** Writing – review & editing. **Giusy Rita Maria La Rosa:** Visualization, Project administration. **Eugenio Pedullà:** Resources, Project administration.

Declaration of competing interest

The authors declare that they have no known competing financial interests or personal relationships that could have appeared to influence the work reported in this paper.

Acknowledgements

The authors would thank Graphenano Dental, New Ancorvis (in the figure of Fabio Ferri) and Rhein 83 (in the figures of Claudio De Angelis and Riccardo Baldari) for their support in the study. The authors would also thank Marco Ortensi CDT for the digital design of the samples used

in the study.

Supplementary materials

Supplementary material associated with this article can be found, in the online version, at [doi:10.1016/j.jdent.2024.104865](https://doi.org/10.1016/j.jdent.2024.104865).

References

- [1] K.J. Anusavice, C. Shen, H.R. Rawls, Phillips' *Science of Dental Materials*, 12th edition, Elsevier Health Sciences, 2012.
- [2] A. Baldi, M. Carossa, A. Comba, M. Alovisei, F. Femiano, D. Pasqualini, E. Berutti, N. Scotti, Wear behaviour of polymer-infiltrated network ceramics, lithium disilicate and cubic zirconia against enamel in a bruxism-simulated scenario, *Biomedicines*. 10 (2022) 1682, <https://doi.org/10.3390/biomedicines10071682>.
- [3] B. Stawarczyk, A. Ender, A. Trottmann, M. Özcan, J. Fischer, C.H.F. Hämmerle, Load-bearing capacity of CAD/CAM milled polymeric three-unit fixed dental prostheses: effect of aging regimens, *Clin. Oral Investig.* 16 (2012) 1669–1677, <https://doi.org/10.1007/s00784-011-0670-4>.
- [4] K. Bataineh, M. Al Janaideh, L.A. Abu-Naba'a, Fatigue resistance of 3-unit CAD-CAM ceramic fixed partial dentures: an FEA study, *Journal of Prosthodontics* 31 (2022) 806–814, <https://doi.org/10.1111/jopr.13487>.
- [5] M.A. Hawthorn, B.R. Chrcanovic, C. Larsson, Long-term retrospective clinical study of tooth-supported fixed partial dentures: a multifactorial analysis, *J. Prosthodont. Res.* 67 (2023) 238–245, https://doi.org/10.2186/jpr.JPR_D_21_00222.
- [6] I. Sailer, N.A. Makarov, D.S. Thoma, M. Zwahlen, B.E. Pjetursson, All-ceramic or metal-ceramic tooth-supported fixed dental prostheses (FDPs)? A systematic review of the survival and complication rates. Part I: single crowns (SCs), *Dental Materials* 31 (2015) 603–623, <https://doi.org/10.1016/j.dental.2015.02.011>.
- [7] Y. Zhou, W. Wei, J. Yan, W. Liu, N. Li, H. Li, S. Xu, Microstructures and metal-ceramic bond properties of Co-Cr biomedical alloys fabricated by selective laser melting and casting, *Materials Science and Engineering: A* 759 (2019) 594–602, <https://doi.org/10.1016/j.msea.2019.05.085>.
- [8] P. Svanborg, L. Hjalmarsson, A systematic review on the accuracy of manufacturing techniques for cobalt chromium fixed dental prostheses, *Biomater. Investig. Dent.* 7 (2020) 31–40, <https://doi.org/10.1080/26415275.2020.1714445>.
- [9] Y. Zhou, X. Dong, N. Li, J. Yan, Effects of post-treatment on metal-ceramic bond properties of selective laser melted Co-Cr dental alloy. Part 1: annealing temperature, *J. Prosthet. Dent.* 129 (2023) 657.e1, <https://doi.org/10.1016/j.prosdent.2022.11.029>. -657.e9.
- [10] J. Li, C. Chen, J. Liao, L. Liu, X. Ye, S. Lin, J. Ye, Bond strengths of porcelain to cobalt-chromium alloys made by casting, milling, and selective laser melting, *J. Prosthet. Dent.* 118 (2017) 69–75, <https://doi.org/10.1016/j.prosdent.2016.11.001>.
- [11] M.S. Zafar, Prosthodontic Applications of Polymethyl Methacrylate (PMMA): an update, *Polymers*. (Basel) 12 (2020) 2299, <https://doi.org/10.3390/polym12102299>.
- [12] J.H. Jorge, E.T. Giampaolo, A.L. Machado, C.E. Vergani, Cytotoxicity of denture base acrylic resins: a literature review, *J. Prosthet. Dent.* 90 (2003) 190–193, [https://doi.org/10.1016/s0022-3913\(03\)00349-4](https://doi.org/10.1016/s0022-3913(03)00349-4).
- [13] C.Y.K. Lung, B.W. Darvell, Minimization of the inevitable residual monomer in denture base acrylic, *Dent. Mater.* 21 (2005) 1119–1128, <https://doi.org/10.1016/j.dental.2005.03.003>.
- [14] H. Matsuo, H. Suenaga, M. Takahashi, O. Suzuki, K. Sasaki, N. Takahashi, Deterioration of polymethyl methacrylate dentures in the oral cavity, *Dent. Mater. J.* 34 (2015) 234–239, <https://doi.org/10.4012/dmj.2014-089>.
- [15] D.R. Haselton, A.M. Diaz-Arnold, M.A. Vargas, Flexural strength of provisional crown and fixed partial denture resins, *J. Prosthet. Dent.* 87 (2002) 225–228, <https://doi.org/10.1067/mpd.2002.121406>.
- [16] H.J. Busscher, M. Rinastiti, W. Siswomihardjo, H.C. van der Mei, Biofilm formation on dental restorative and implant materials, *J. Dent. Res.* 89 (2010) 657–665, <https://doi.org/10.1177/0022034510368644>.
- [17] F. Grande, F. Tesini, M.C. Pozzan, E.M. Zamperoli, M. Carossa, S. Catapano, Comparison of the accuracy between denture bases produced by subtractive and additive manufacturing methods: a pilot study, *Prosthesis* 4 (2022) 151–159, <https://doi.org/10.3390/prosthesis4020015>.
- [18] E.E. Totu, A.C. Nechifor, G. Nechifor, H.Y. Aboul-Enein, C.M. Cristache, Poly (methyl methacrylate) with TiO₂ nanoparticles inclusion for stereolithographic complete denture manufacturing - the future in dental care for elderly edentulous patients? *J. Dent.* 59 (2017) 68–77, <https://doi.org/10.1016/j.jdent.2017.02.012>.
- [19] N. Turagam, D.P. Mudrakola, Effect of micro-additions of carbon nanotubes to polymethylmethacrylate on reduction in polymerization shrinkage, *J. Prosthodont.* 22 (2013) 105–111, <https://doi.org/10.1111/j.1532-849X.2012.00917.x>.
- [20] S.V. Agarwalla, R. Malhotra, V. Rosa, Translucency, hardness and strength parameters of PMMA resin containing graphene-like material for CAD/CAM restorations, *J. Mech. Behav. Biomed. Mater.* 100 (2019) 103388, <https://doi.org/10.1016/j.jmbm.2019.103388>.
- [21] M. Punset, A. Brizuela, E. Pérez-Pevida, M. Herrero-Climent, J.M. Manero, J. Gil, Mechanical characterization of dental prostheses manufactured with PMMA-graphene composites, *Materials* 15 (2022) 5391, <https://doi.org/10.3390/ma15155391>.
- [22] V. Bharath, V. Auradi, G.B.V. Kumar, M. Nagaral, M. Chavali, M. Helal, R. Sami, N. I. Aljuraide, J.W. Hu, A.M. Galal, Microstructural evolution, tensile failure, fatigue behavior and wear properties of Al₂O₃ reinforced Al2014 alloy T6 heat treated metal composites, *Materials*. (Basel) 15 (2022) 4244, <https://doi.org/10.3390/ma15124244>.
- [23] C. Bacali, I. Baldea, M. Moldovan, R. Carpa, D.E. Olteanu, G.A. Filip, V. Nastase, L. Lascu, M. Badea, M. Constantiniu, F. Badea, Flexural strength, biocompatibility, and antimicrobial activity of a polymethyl methacrylate denture resin enhanced with graphene and silver nanoparticles, *Clin. Oral Investig.* 24 (2020) 2713–2725, <https://doi.org/10.1007/s00784-019-03133-2>.
- [24] L. Azevedo, J.L. Antonaya-Martin, P. Molinero-Mourelle, J. Del Río-Highsmith, Improving PMMA resin using graphene oxide for a definitive prosthodontic rehabilitation - A clinical report, *J. Clin. Exp. Dent.* 11 (2019) e670–e674, <https://doi.org/10.4317/jced.55883>.
- [25] C. Bacali, M. Badea, M. Moldovan, C. Sarosi, V. Nastase, I. Baldea, R.S. Chiorean, M. Constantiniu, The influence of graphene in improvement of physico-mechanical properties in PMMA denture base resins, *Materials*. (Basel) 12 (2019) 2335, <https://doi.org/10.3390/ma12142335>.
- [26] X. Li, X. Liang, Y. Wang, D. Wang, M. Teng, H. Xu, B. Zhao, L. Han, Graphene-based nanomaterials for dental applications: principles, current advances, and future outlook, *Front. Bioeng. Biotechnol.* 10 (2022). <https://www.frontiersin.org/articles/10.3389/fbioe.2022.804201>. accessed December 27, 2023.
- [27] J.-H. Lee, J.-K. Jo, D.-A. Kim, K.D. Patel, H.-W. Kim, H.-H. Lee, Nano-graphene oxide incorporated into PMMA resin to prevent microbial adhesion, *Dent. Mater.* 34 (2018) e63–e72, <https://doi.org/10.1016/j.dental.2018.01.019>.
- [28] J. Chen, H. Peng, X. Wang, F. Shao, Z. Yuan, H. Han, Graphene oxide exhibits broad-spectrum antimicrobial activity against bacterial phytopathogens and fungal conidia by intertwining and membrane perturbation, *Nanoscale* 6 (2014) 1879–1889, <https://doi.org/10.1039/c3nr04941h>.
- [29] I. Nedeljkovic, J. De Munck, V. Slomka, B. Van Meerbeek, W. Teughels, K.L. Van Landuyt, Lack of buffering by composites promotes shift to more cariogenic bacteria, *J. Dent. Res.* 95 (2016) 875–881, <https://doi.org/10.1177/0022034516647677>.
- [30] F.H. van de Sande, N.J.M. Opdam, G.J. Truin, E.M. Bronkhorst, J.J. de Soet, M. S. Cenci, M.-C. Huysmans, The influence of different restorative materials on secondary caries development in situ, *J. Dent.* 42 (2014) 1171–1177, <https://doi.org/10.1016/j.jdent.2014.07.003>.
- [31] M. Bourbia, D. Ma, D.G. Cvitkovich, J.P. Santerre, Y. Finer, Cariogenic bacteria degrade dental resin composites and adhesives, *J. Dent. Res.* 92 (2013) 989–994, <https://doi.org/10.1177/0022034513504436>.
- [32] C. Lopez-Suarez, C. Tobar, M.F. Sola-Ruiz, J. Pelaez, M.J. Suarez, Effect of thermomechanical and static loading on the load to fracture of metal-ceramic, monolithic, and veneered zirconia posterior fixed partial dentures, *J. Prosthodont.* 28 (2019) 171–178, <https://doi.org/10.1111/jopr.13008>.
- [33] C. Lopez-Suarez, V. Rodriguez, J. Pelaez, R. Agustín-Panadero, M.J. Suarez, Comparative fracture behavior of monolithic and veneered zirconia posterior fixed dental prostheses, *Dent. Mater. J.* 36 (2017) 816–821, <https://doi.org/10.4012/dmj.2016-391>.
- [34] M.J. Ambré, F. Aschan, P.V. von Steyern, Fracture Strength of Yttria-Stabilized Zirconium-Dioxide (Y-TZP) Fixed Dental Prostheses (FDPs) with Different Abutment Core Thicknesses and Connector Dimensions, *Journal of Prosthodontics* 22 (2013) 377–382, <https://doi.org/10.1111/jopr.12003>.
- [35] L. Trebbi, G. di Febo, G. Carnevale, A technique to obtain a precise functional occlusion using porcelain fused to gold, *Int. J. Periodontics Restorative Dent.* 2 (1982) 44–57.
- [36] DIN ISO 48-4:2021-02 - UNI Ente Italiano di Normazione, (n.d.). <https://store.uni.com/din-iso-48-4-2021-02> (accessed November 9, 2023).
- [37] ISO 5833 : implants for Surgery - Acrylic Resin Cements, (n.d.). https://global.ihb.com/doc_detail.cfm?document_name=ISO%205833&item_s_key=00143434 (accessed November 9, 2023).
- [38] UNI EN ISO 20795-1:2013 - UNI Ente Italiano di Normazione, (n.d.). <https://store.uni.com/uni-en-iso-20795-1-2013> (accessed November 9, 2023).
- [39] S. Catapano, M. Ferrari, N. Mobilio, M. Montanari, M. Corsalini, F. Grande, Comparative analysis of the stability of prosthetic screws under cyclic loading in implant prosthodontics: an in vitro study, *Applied Sciences* 11 (2021) 622, <https://doi.org/10.3390/app11020622>.
- [40] M.C. Pozzan, F. Grande, E. Mochi Zamperoli, F. Tesini, M. Carossa, S. Catapano, Assessment of preload loss after cyclic loading in the OT bridge system in an “all-on-four” rehabilitation model in the absence of one and two prosthesis screws, *Materials*. (Basel) 15 (2022) 1582, <https://doi.org/10.3390/ma15041582>.
- [41] M. Özcan, Fracture reasons in ceramic-fused-to-metal restorations, *J. Oral Rehabil.* 30 (2003) 265–269, <https://doi.org/10.1046/j.1365-2842.2003.01038.x>.
- [42] A.C. Ionescu, E. Brambilla, P.M. Pires, A. López-Castellano, A.M. Alambiaga-Caravaca, C. Lenardi, S. Sauro, Physical-chemical and microbiological performances of graphene-doped PMMA for CAD/CAM applications before and after accelerated aging protocols, *Dent. Mater.* 38 (2022) 1470–1481, <https://doi.org/10.1016/j.dental.2022.06.032>.
- [43] H. Kim, A.A. Abdala, C.W. Macosko, Graphene/Polymer Nanocomposites, *Macromolecules*. 43 (2010) 6515–6530, <https://doi.org/10.1021/ma100572e>.
- [44] G. Gonçalves, P.A.A.P. Marques, A. Barros-Timmons, I. Bdkin, M.K. Singh, N. Emami, J. Grácio, Graphene oxide modified with PMMA via ATRP as a reinforcement filler, *J. Mater. Chem.* 20 (2010) 9927–9934, <https://doi.org/10.1039/C0JM01674H>.
- [45] J.L. Ferracane, Hygroscopic and hydrolytic effects in dental polymer networks, *Dent. Mater.* 22 (2006) 211–222, <https://doi.org/10.1016/j.dental.2005.05.005>.

- [46] S. Ito, M. Hashimoto, B. Wadgaonkar, N. Svizero, R.M. Carvalho, C. Yiu, F. A. Rueggeberg, S. Foulger, T. Saito, Y. Nishitani, M. Yoshiyama, F.R. Tay, D. H. Pashley, Effects of resin hydrophilicity on water sorption and changes in modulus of elasticity, *Biomaterials* 26 (2005) 6449–6459, <https://doi.org/10.1016/j.biomaterials.2005.04.052>.
- [47] F. Grande, M. Carossa, A. Balma, N. Scotti, F. Mussano, S. Catapano, Influence of thickness and thermocycling on tensile strength of two resin-based cements used for overdenture bar-type attachments: an in vitro study, *IJP* (2023), <https://doi.org/10.11607/ijp.8673>.
- [48] S. Shahrabaf, R. van Noort, B. Mirzakouchaki, E. Ghassemieh, N. Martin, Fracture strength of machined ceramic crowns as a function of tooth preparation design and the elastic modulus of the cement, *Dental Materials* 30 (2014) 234–241, <https://doi.org/10.1016/j.dental.2013.11.010>.
- [49] K.T.A. Tavano, A.M. Botelho, D.W. Douglas-de-Oliveira, A.F. Avila, R. Huebner, Resistance to fracture of intraradicular posts made of biological materials, *BMC Oral Health* 20 (2020) 300, <https://doi.org/10.1186/s12903-020-01295-0>.
- [50] N.K. Singh, E. Cadoni, M.K. Singha, N.K. Gupta, Dynamic tensile behavior of multi phase high yield strength steel, *Mater. Des.* 32 (2011) 5091–5098, <https://doi.org/10.1016/j.matdes.2011.06.027>.
- [51] A.S. Rizkalla, D.W. Jones, Indentation fracture toughness and dynamic elastic moduli for commercial feldspathic dental porcelain materials, *Dental Materials* 20 (2004) 198–206, [https://doi.org/10.1016/S0109-5641\(03\)00092-7](https://doi.org/10.1016/S0109-5641(03)00092-7).
- [52] C.K.Y. Yiu, N.M. King, D.H. Pashley, B.I. Suh, R.M. Carvalho, M.R.O. Carrilho, F. R. Tay, Effect of resin hydrophilicity and water storage on resin strength, *Biomaterials* 25 (2004) 5789–5796, <https://doi.org/10.1016/j.biomaterials.2004.01.026>.
- [53] U. Ortengren, F. Andersson, U. Elgh, B. Terselius, S. Karlsson, Influence of pH and storage time on the sorption and solubility behaviour of three composite resin materials, *J. Dent.* 29 (2001) 35–41, [https://doi.org/10.1016/S0300-5712\(00\)00055-5](https://doi.org/10.1016/S0300-5712(00)00055-5).
- [54] C. Vallés, D.G. Papageorgiou, F. Lin, Z. Li, B.F. Spencer, R.J. Young, I.A. Kinloch, PMMA-grafted graphene nanoplatelets to reinforce the mechanical and thermal properties of PMMA composites, *Carbon*. N. Y. 157 (2020) 750–760, <https://doi.org/10.1016/j.carbon.2019.10.075>.
- [55] C. Yilmaz, T. Korkmaz, The reinforcement effect of nano and microfillers on fracture toughness of two provisional resin materials, *Mater. Des.* 28 (2007) 2063–2070, <https://doi.org/10.1016/j.matdes.2006.05.029>.
- [56] R. Agustín-Panadero, R. León Martínez, M.F. Solá-Ruíz, A. Fons-Font, G. García Engra, L. Fernández-Estevan, Are metal-free monolithic crowns the present of prosthesis? study of mechanical behaviour, *Materials*. (Basel) 12 (2019) E3663, <https://doi.org/10.3390/ma12223663>.
- [57] H.A. Vidotti, J.R. Pereira, E. Insaurralde, A.L.P.F. de Almeida, A.L. do Valle, Thermo and mechanical cycling and veneering method do not influence Y-TZP core/veneer interface bond strength, *J. Dent.* 41 (2013) 307–312, <https://doi.org/10.1016/j.jdent.2012.12.001>.
- [58] L. Borchers, M. Stiesch, F.-W. Bach, J.-C. Buhl, C. Hübsch, T. Kellner, P. Kohorst, M. Jendras, Influence of hydrothermal and mechanical conditions on the strength of zirconia, *Acta Biomater.* 6 (2010) 4547–4552, <https://doi.org/10.1016/j.actbio.2010.07.025>.
- [59] M. Borba, M.D. de Aratújo, K.A. Fukushima, H.N. Yoshimura, J.A. Griggs, Á. Della Bona, P.F. Cesar, Effect of different aging methods on the mechanical behavior of multi-layered ceramic structures, *Dent. Mater.* 32 (2016) 1536–1542, <https://doi.org/10.1016/j.dental.2016.09.005>.
- [60] T.Y. Marghalani, Frequency of undercuts and favorable path of insertion in abutments prepared for fixed dental prostheses by preclinical dental students, *J. Prosthet. Dent.* 116 (2016) 564–569, <https://doi.org/10.1016/j.prosdent.2016.03.014>.
- [61] P.H. Corazza, S.A. Feitosa, A.L.S. Borges, A.Della Bona, Influence of convergence angle of tooth preparation on the fracture resistance of Y-TZP-based all-ceramic restorations, *Dental Materials* 29 (2013) 339–347, <https://doi.org/10.1016/j.dental.2012.12.007>.
- [62] A. Szczesio-Włodarczyk, J. Sokolowski, J. Kleczewska, K. Bociog, Ageing of dental composites based on methacrylate resins—a critical review of the causes and method of assessment, *Polymers*. (Basel) 12 (2020) 882, <https://doi.org/10.3390/polym12040882>.
- [63] H.T. Shillinburg, et al., *Fundamentals of Fixed Prosthodontics*, Quintessence Publishing Company, 1997 (n.d.).